

Balancing Stability and Stiffness Through Optimization of Parallel Compliance

Mincheol Kim and Ashish D. Deshpande

Abstract—Having a wide range of achievable stiffness is essential for a robotic manipulator to robustly and safely interact with unknown environments. However, the achievable controller stiffness is fundamentally bounded by the system’s passive stiffness, which introduces problems for compliant robots with series elasticity. Since strong passive stiffness is undesirable in uncertain environments, we introduce coupled tendon routing (CTR) along with nonlinear parallel compliance (NPC) to effectively shift this boundary with minimal change to the overall stiffness. In this paper, we present a novel method for optimization and physical implementation to systematically determine the nonlinear parallel compliance to meet stability goals and further reduce the overall stiffness through coupled tendon routing. Experiments are carried out with two tendon-driven 2-DOF planar fingers to demonstrate and validate the effectiveness of the proposed method.

I. INTRODUCTION

Compliance of the human finger plays a crucial role during interaction with unstructured environments. Humans freely adjust their finger stiffness depending on the situation or application, resulting in versatile manipulation. While stiffness control has been implemented in robotic hands [1], exactly how to choose a robot’s inherent or passive stiffness is an open question. High passive stiffness (e.g., industrial manipulators) improves precision but lacks flexibility and may damage the environment, whereas low stiffness (e.g., soft robotic fingers) improves robustness but suffers from inaccuracy. Therefore, modulation of compliance is desirable to complete a variety of manipulation tasks under unknown environment dynamics.

For non-backdrivable actuators to produce compliant motion, the concept of series compliance had been investigated as a replacement for expensive force control using a load cell [2]. However, the employment of series elasticity limits the renderable stiffness boundary [3][4]. Furthermore, increasing the series elasticity can be unsafe in unstructured environments, and the resulting higher bandwidth of the overall system could cause instability in noisy environments [5]. To resolve this issue, parallel actuation or distributed actuation has been introduced in industrial settings [6][7], but these methods inevitably use additional motors which makes the actuation system bulky and unfit for light-weight and compact applications.

Therefore, there needs to be an alternative option to add elasticity to the system instead of solely relying on series elasticity. Parallel compliance (PC) properties are one viable

option to complement the necessary stiffness. Parallel compliance along with series actuation has been implemented by several researchers [8][9]. However, these works only deal with the performance of non-compliant robotic end-effectors under position control and do not investigate nor mathematically formulate the effects of parallel compliance on control stability. Some researchers have used parallel compliance to save energy consumption during periodic motions [10], but periodic motions are not common in dexterous manipulation. Additionally, our aim is to use coupled or nonlinear parallel compliance to achieve stability with minimal stiffness increment.

This manuscript addresses the effects of parallel compliance in tendon-driven robotic hands on stiffness control stability, inspired by the profound effects of joint compliance on human hand performance [11]. In terms of control, incorporation of parallel compliance is an effective yet simple solution towards stability as it introduces no time delay to the system and only needs a feed-forward term in the control input. Parallel compliance can simply be installed in tendon-driven systems by adding extension springs along with pulleys at the joint-level without interfering with existing tendons.

This paper demonstrates, for the first time, the optimization process and stabilization effects of coupled and nonlinear PC and proposes the possibility of minimizing the size, weight, and cost of the overall actuation system with a stiffness-efficient design. With this outcome, it is possible to stably render a wide range of stiffness without using power-demanding motors or higher series stiffness, which can be convenient in various problems such as dexterous manipulation in unknown environments. Section II will explain passivity-based stability criteria under stiffness control. Section III will introduce the optimization method, underlining the importance of off-diagonal terms and configuration-dependency. Then, we will show simulation results that achieve a significant reduction from previous work [12] in stiffness through coupled tendon routing (CTR) along with the overall optimization process. In experiments, we show that further reduction is possible by introduction of nonlinear parallel compliance (NPC). Section IV will discuss some of the important remarks from the results, and conclusions will be drawn in Section V.

II. STIFFNESS CONTROL STABILITY

In order to maintain passivity of the overall system and mechanically ensure the system returns to its equilibrium state, the controller stiffness should not exceed the passive stiffness of the robot [3][4]. This limits the range of stiffness values

M. Kim and A.D. Deshpande are with the Department of Mechanical Engineering University of Texas at Austin, Austin, TX 78712. mincheol@utexas.edu and ashish@austin.utexas.edu

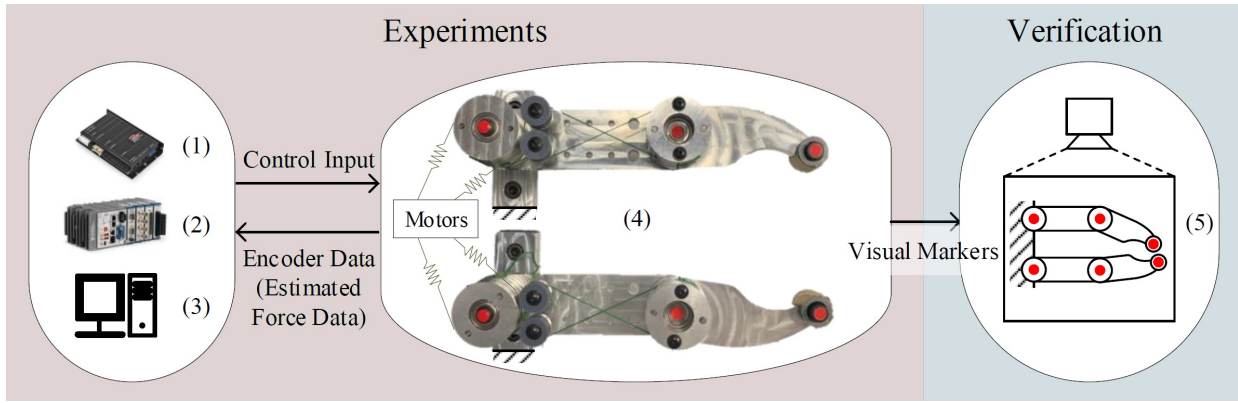


Fig. 1. The NuFingers: a set of 2-DOF tendon-driven robotic fingers (4) for experimental validation. Brushed DC motors are closed-loop position-controlled by EPOS2 50/5 (1) and connected to the tendons via springs acting as series elastic actuators using the encoders. Communication between the controller and the PC (3) is supported by an NI-cRIO (2). While stiffness control was performed using proprioceptive sensors in real time, we used joint positions extracted from a post-processed image data (5) from a camera for verification.

that a robotic system can stably realize, thereby limiting the type of tasks that the system is able to carry out. Work in [12] demonstrates that adding parallel compliance to the system is a good option to shift the upper bound of the stable range. In this research, we show that optimal passive stiffness is achievable by nonlinear parallel compliance and coupled tendon routing between joints. This enables the system to perform tasks that require lower stiffness and also reduces actuator effort.

For tendon-driven robotic fingers, the passivity-based stability criteria can be formulated as follows [12]:

$$\mathbf{J}^{-T} \mathbf{K}_{pc} \mathbf{J}^{-1} \leq \mathbf{K}_{x,d} \leq \mathbf{K}_{x,passive} \quad (1)$$

where $\mathbf{K}_{x,passive}$ and $\mathbf{K}_{x,d}$ denote the system's passive and desired Cartesian stiffness matrices respectively, \mathbf{J} is the Jacobian, and \mathbf{K}_{pc} represents the parallel compliance matrix.

$$\mathbf{K}_{x,passive} = \mathbf{J}^{-T} (\mathbf{R}^T \mathbf{K}_{sc} \mathbf{R} + \mathbf{K}_{pc} - \mathbf{K}_{j,CCT}) \mathbf{J}^{-1} \quad (2)$$

$\mathbf{K}_{x,passive}$ is defined above, where \mathbf{R} and \mathbf{K}_{sc} denote the routing and series compliance matrices respectively, and $\mathbf{K}_{j,CCT}$ refers to the external force based stiffness term [13]. As seen from Eq. (1), the addition of the parallel compliance term \mathbf{K}_{pc} influences both lower and upper boundaries of the passivity range. Therefore, as long as the desired stiffness is known throughout the task, the optimal form of parallel compliance can be determined through convex optimization.

III. OPTIMIZATION OF PARALLEL COMPLIANCE

The overall stiffness of the end-effector as well as the torque requirements all depend heavily on \mathbf{K}_{pc} as suggested by Eq. (2). Therefore, it is crucial to formulate an optimization problem to identify the amount of PC that strikes the balance between the necessary stiffness and stability. Note that this method can be extended to other physical configurations with different tendon routing strategies or link lengths. From the optimization, we seek to determine \mathbf{K}_{pc} for a predefined task environment and synthesize the linear and nonlinear PCs that will physically realize this \mathbf{K}_{pc} .

Work in [12] investigated the possibility of using linear PCs to adjust the stable range of stiffness. However, it is rare to

find characteristics that are purely linear and decoupled from one another as dealt in [12]. For instance, it is easy to see human fingers exhibit highly coupled and nonlinear passive compliances depending on their configuration. In this study, notable improvements have been made: we introduce nonlinear parallel compliance (NPC) along with coupled tendon routing (CTR) that stabilizes the system with minimal change to the overall stiffness. Through simulation and experiments using the NuFingers shown in Fig. 1, this paper will demonstrate the validity and effectiveness of the proposed method.

A. Optimization

To satisfy the stability criteria throughout n points in a given workspace while minimizing the resultant overall stiffness, the fully-populated \mathbf{K}_{pc} is optimized by a multi-object search algorithm based on interior-point methods [14]. One can relate the matrix inequalities shown in Eq. (1) to the size comparison of the hyperellipsoids represented by the matrices regardless of the number of dimensions.

To avoid unnecessary stiffness, however, the cost function was defined as the Frobenius norm of \mathbf{K}_{pc} since it is desirable to minimize the area of the stiffness ellipse. By trimming out the excess stiffness, we can also minimize the chance of damaging the unknown environment as well as reduce motor effort.

The optimization problem is set up below.

$$\begin{aligned} \min \quad & \|\mathbf{K}_{pc}(q_i)\|_F \\ \text{s.t.} \quad & \text{Re}(\lambda_i(\mathbf{K}_{x,passive} - \mathbf{K}_{x,d})) \geq \epsilon, \\ & \mathbf{K}_{x,passive} = \mathbf{K}_{x,passive}(\mathbf{J}, \mathbf{K}_{sc}, \mathbf{R}, \mathbf{K}_{pc}, \mathbf{f}_{ext}(\alpha)) \quad (3) \\ & i = 1, \dots, n \\ & \alpha = -30^\circ, \dots, 30^\circ. \end{aligned}$$

Here, \mathbf{f}_{ext} , α , and ϵ represent the interaction force exerted at the fingertip, the angle of the force with respect to the horizontal axis, and a small positive real number to avoid singularity on eigenvalues. λ_i represents the eigenvalues of the matrix argument at the i -th point.

During this process, passive stiffness matrices at n points from the workspace with the external force exerted at every

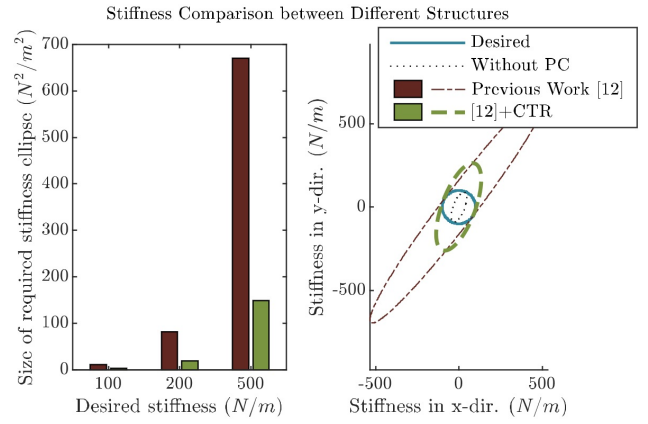
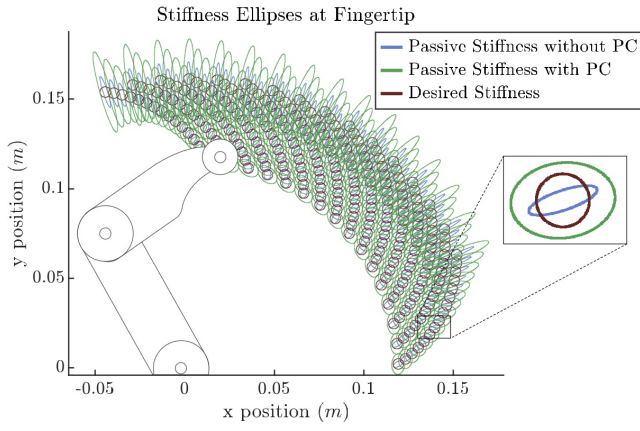


Fig. 2. (Left) \mathbf{K}_{pc} is optimized about the 256 sample configurations from the workspace. We can observe that passive stiffness ellipses without PC are initially smaller than desired stiffness ellipses, inferring the loss of passivity. After the addition of PC, the system recovers the passivity, successfully satisfying the positive definiteness constraint in Eq. (1). Stiffness comparison between coupled and decoupled \mathbf{K}_{pc} are also shown. (Middle) The coupled tendon routing (CTR) strategy produces significantly smaller stiffness ellipses compared to the approach used in [12]. (Right) Visual representation of the overall stiffness with different structures is shown. Desired stiffness is $100 N/m$.

angle are concatenated together. From our simulation, we needed sufficient samples to curve-fit the results to synthesize actual PC components. We heuristically found it suffices to use $16 \times 16 = 256$ points from the workspace and an angular resolution of 30° for the interaction force. This number is chosen based on the range of interaction angles during the object manipulation experiments to make certain that the synthesized PC covers the entire range of motion. Details of the optimization procedures can be found in [14]. In [12], \mathbf{K}_{pc} was constant across the workspace and not allowed to have off-diagonal terms, making it fully linear and decoupled across the joints.

By allowing \mathbf{K}_{pc} to have non-zero off-diagonal terms, i.e., coupled tendon routing, we can relax the optimization constraints and thus further reduce the stiffness of \mathbf{K}_{pc} . The results are visualized in Fig. 2 for a case with desired Cartesian stiffness of $70 N/m$ and interaction force of $1.5 N$. With fully coupled \mathbf{K}_{pc} , the passive stiffness ellipses successfully enclose the desired stiffness ellipses, satisfying the passivity conditions shown in Eq. (1).

B. Simulation

For simulation in MATLAB, we used the parameters of NuFingers given by CAD software and a rise time of $0.012s$, which the maxon EPOS2 controller was tuned to accomplish. The right of Fig. 2 shows the visual representations of the optimization results under different physical setups. The bar graph represents the areas of the passive stiffness ellipses depending on the setup. The ellipses represent the robot's passive stiffness, desired stiffness, and overall stiffness after the addition of parallel compliance under different structures. As expected, the area of the ellipse is significantly smaller with coupled PC routing strategy. Generally, less stiff mechanisms are favorable in unstructured environments to gracefully handle unforeseen collisions.

Figure 3 depicts the step response (i.e., desired and actual positions of the end-effector) over time with a desired isometric stiffness of $100 N/m$. First, we verified that the

system cannot render the desired stiffness without PC due to the loss of passivity (Fig. 3a). As soon as the step input is given, the manipulator diverges. We then added the parallel compliance obtained from Fig. 2, and the system's stability profoundly improved under the same conditions (Fig. 3b,c). Note that i) the overall control scheme is identical, and ii) the area of the overall stiffness is about 70% smaller when we allowed \mathbf{K}_{pc} to be fully populated. From these simulation results, we can safely conclude that the employment of PC successfully stabilizes the system and the coupled routing strategy results in significant reduction of overall stiffness. For experiments, we adopt the NPC to vary the stiffness according to the configuration in addition to the CTR strategy.

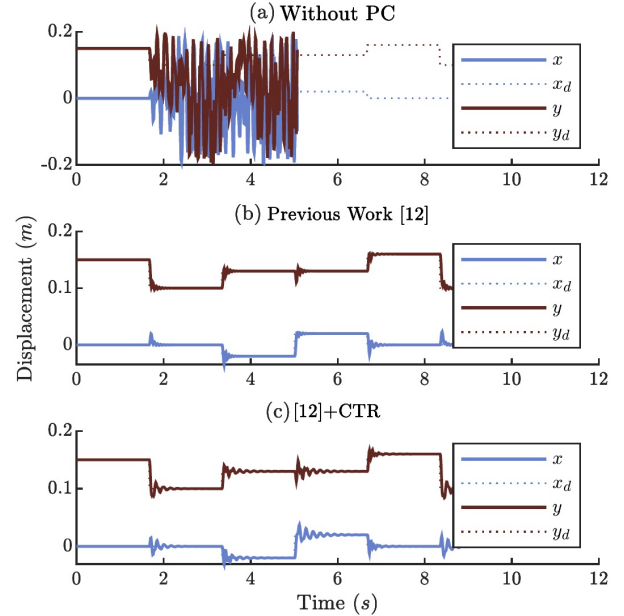


Fig. 3. Step responses of the system with different physical setups are shown: (a) without PC, (b) decoupled \mathbf{K}_{pc} [12], and (c) coupled \mathbf{K}_{pc} are shown. The desired isometric Cartesian stiffness is $100 N/m$. Without PC the system quickly goes unstable whereas addition of PC greatly improves the overall stability. Note that coupled PC achieves stability with lower overall stiffness, which is convenient for manipulation in uncertain environments.

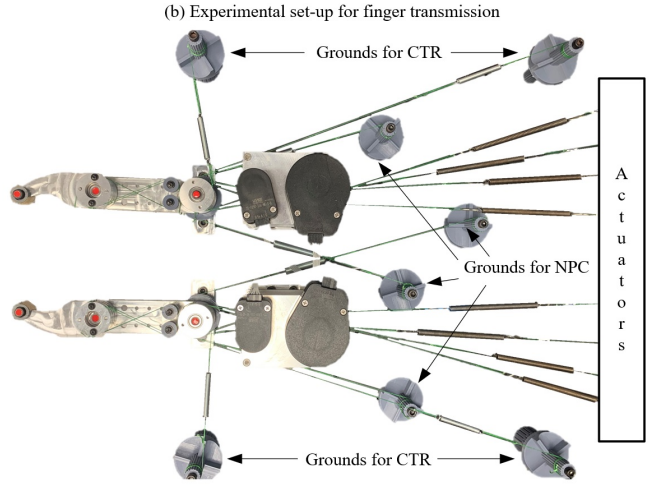
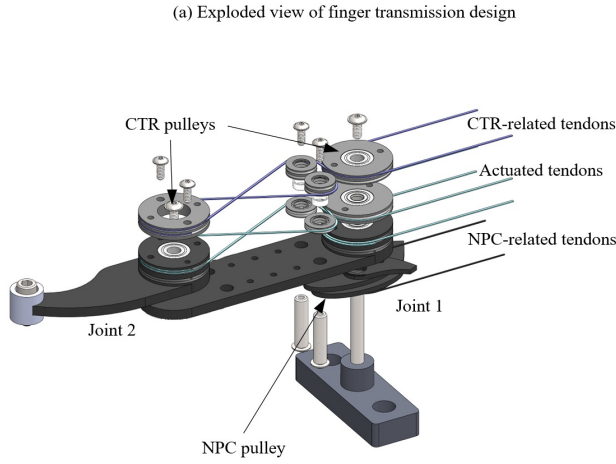


Fig. 4. Tendon routing for the proposed structure. (a) In the proposed setup, there are two notable changes from [12]. The top layer uses coupled tendon routing (CTR) that accounts for the off-diagonal terms in \mathbf{K}_{pc} . In addition, nonlinear parallel compliance (NPC) in the bottom layer provides optimized stiffness that depends on the finger configuration. (b) Actual set-up of the mechanism is shown. Note that all tendons are connected to linear extension springs.

C. Experiments

We designed NuFingers as shown in Fig. 1,4 to conduct experimental validation. Three scenarios shown in Fig. 5 are considered. The first scenario involves a single finger with step inputs in Cartesian space, while the second and third scenarios involve two fingers grasping and moving an object either in steps or in a continuous elliptical trajectory.

In the experiments, the desired Cartesian stiffness is set to 70 N/m for single finger steps and the object-space stiffness is set to 140 N/m for two-fingered object manipulation. Both stiffnesses are isometric to avoid complications but note that this can be defined arbitrarily so long as the system remains passive. These values are chosen based on the inherent passive stiffness of our system from series compliance and the capacity of the motors used (Maxon A-max 32, 353239).

We implement a vision system in addition to the proprioceptive encoder measurements to validate our data with more accurate and reliable measurements. A 4K camera is installed above the NuFingers testbed as seen in Fig. 1 and records the response of the robot at 60 FPS. Later, videos are post-processed in MATLAB to extract visual marker positions and calculate joint displacements at each frame.

As shown in Fig. 2, the required stiffness of PC heavily depends on the tendon routing strategy. However, it is also affected by the configuration of the finger due to the Jacobian in Eq. (2). Therefore, instead of using a fixed-radius pulley as in [12], stiffness can further be reduced through nonlinear \mathbf{K}_{pc} across the workspace. We also take note that the previous approach [12] alone is infeasible due to the physical size constraints of NuFingers, which disallow installation of springs with the required high stiffness for [12] shown in Table I. Instead, we adopt NPC along with the previous approach for performance comparison.

Here, we use the extended methodology [15] to synthesize NPC and generate nonlinear stiffness \mathbf{K}_{pc} using an antagonistic pair of extension springs. Note that in addition to

NPC, our proposed setup also uses a CTR strategy for parallel compliance.

After careful examination, we have found that configuration-dependent change in optimal stiffness occurs primarily in the first joint. Hence, we choose to synthesize the NPC associated with the first joint and additionally introduce CTR on top of the entire mechanism, as shown in Fig. 4. In the next section, we derive the stiffness of the extension springs attached to the antagonistic pairs based on the structure of the mechanism using the optimization results from Eq. (3).

1) *Computation of Extension Spring Stiffness:* In the proposed structure, we utilize two different sets of torques to impose the required stiffness \mathbf{K}_{pc} : nonlinear torques applied at the first joint, and the additional coupled torques on top. Details of the physical structure of the mechanism are shown in Fig. 4. The resulting torques from this configuration can be expressed as:

$$\boldsymbol{\tau} = \begin{bmatrix} \tau_1 \\ \tau_2 \end{bmatrix} = \begin{bmatrix} \tau_{nl} + 2k_c r_c^2 ((q_1 - q_{10}) + (q_2 - q_{20})) \\ 2k_c r_c^2 ((q_1 - q_{10}) + (q_2 - q_{20})) \end{bmatrix} \quad (4)$$

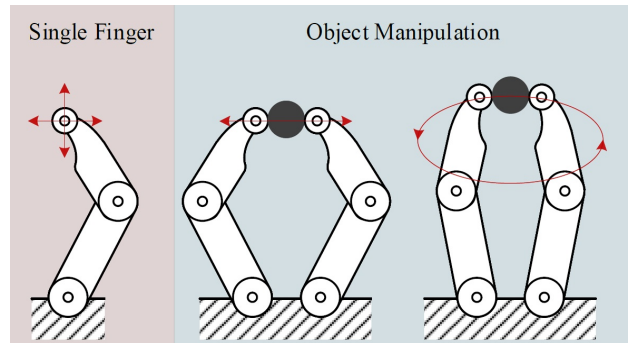


Fig. 5. The proposed structure (NPC + CTR) is validated through a set of experiments in Cartesian space: (left) Scenario 1: step input to a single finger; (middle and right) Scenario 2 and 3: object manipulation with two fingers.

where τ_{nl} , k_c , and r_c represent torque from the NPC, the extension spring stiffness, and the moment arm for the coupled PC tendons, respectively. Each joint's current and equilibrium positions are represented as q_1 , q_2 , q_{10} , and q_{20} . Based on the definition of the joint stiffness, the stiffness matrix is the partial derivative of joint torques:

$$\mathbf{K}_{pc} = \frac{\partial \boldsymbol{\tau}}{\partial \mathbf{q}} = \begin{bmatrix} \frac{d}{dq_1}(\tau_{nl}) + 2k_c r_c^2 & 2k_c r_c^2 \\ 2k_c r_c^2 & 2k_c r_c^2 \end{bmatrix} \quad (5)$$

This is the overall stiffness matrix for the mechanism. Notice that only the nonlinear element $\frac{d}{dq_1}(\tau_{nl})$ varies throughout the workspace. Therefore, we carried out the optimization process shown in Eq. (3) with a constraint that \mathbf{K}_{pc} takes the form of Eq. (5). Next, k_c and $\frac{d}{dq_1}(\tau_{nl})$ are computed from the optimization results. The radius of the moment arms r_c is designed to be the same as actuated joint radius ($18.75mm$) for the sake of manufacturing simplicity. The optimization results from various approaches for a given point in the workspace are compared in Fig. 6. As expected, the approach used in [12] produces the stiffest PC and a more compliant result can be acquired through NPC. The stiffness gets reduced further with the coupled tendon routing strategy, which is the proposed method.

From the optimized \mathbf{K}_{pc} , we compute k_c using Eq. (5) since r_c is known. Then $\frac{d}{dq_1}(\tau_{nl})$ can be computed point-wise and curve-fitted, leading us to τ_{nl} from integration. We can use τ_{nl} to synthesize a nonlinear pulley profile that imposes the desired joint stiffness [15]. This pulley will act as a nonlinear torsional spring. Note that the degree of nonlinearity depends heavily on multiple variables shown in Eq. (3). Similarly, an additional nonlinear pulley profile is generated to see the performance of [12] + NPC. One of the advantages of utilizing PC to stabilize the system is that it can be modeled as an additional feedforward actuator effort without any changes in

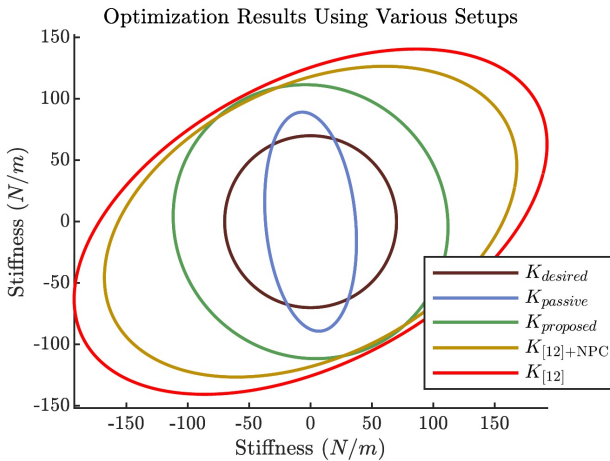


Fig. 6. \mathbf{K}_{pc} is optimized based on the criteria shown in Eq. (3) for different setups as stated in the subscripts. The desired Cartesian stiffness is $70 N/m$. As expected, the previous work [12] results in the stiffest \mathbf{K}_{pc} . The NPC alleviates the high stiffness, and coupled tendon routing (CTR) further reduces the stiffness. The proposed structure incorporates NPC + CTR and thus produces the most stiffness-efficient results.

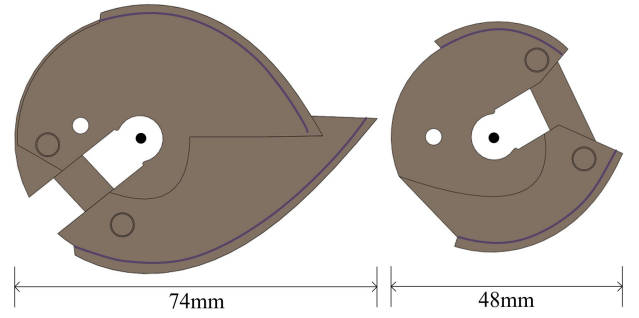


Fig. 7. Nonlinear pulley profiles are generated based on the optimal stiffness to ensure stability for each configuration in the workspace. The desired stiffness is set to $70 N/m$. (Left) Nonlinear pulley profile combined with the previous approach ([12]+NPC). (Right) Nonlinear pulley profile for the proposed method (NPC + CTR).

the control loop. We utilize the extended methodology [15] by using the torque profile τ_{nl} to generate the pulleys depicted in Fig. 7.

Table I shows the necessary stiffness of extension springs based on the optimization results for $70 N/m$. We can see that NPC by itself significantly reduces the stiffness of the required springs compared to the previous approach. In the proposed structure, where NPC and CTR are employed together, the stiffness of the extension springs is further minimized. Notice that the maximum moment arm of the proposed structure is about 50% smaller than [12]+NPC, making it preferable in compact settings.

2) *Experiment Results:* For experiments, we installed the synthesized NPC along with linear extension springs based on the given structures. However, due to the size constraints of the extension springs, we could not find proper springs that satisfy Table I and fit our mechanism for the approach taken in [12]. Therefore, for the experiments, we only compare the previous approach combined with NPC and the proposed approach. We carefully examined the results to draw a reasonable conclusion about the performance difference between the proposed and past [12] approaches. The step response and elliptical trajectory tracking results using NuFingers are shown in Fig. 8. As the results suggest, the system is unable to render high controller stiffness without any PC and quickly diverges. Consistent with the simulation results, stability is recovered with the addition of parallel compliance. Both structures enable the system to quickly converge to the equilibrium configurations.

From the experiments, we verified that the desired trajectories can be stably tracked using the proposed structure (NPC

TABLE I
PHYSICAL PARAMETERS FOR DIFFERENT STRUCTURES.

Joints	Structure	Stiffness (N/m)	Moment Arm (mm)
1	[12]	1548.04	18.75
2		534.57	18.75
1	[12] + NPC	749.54	26.7 – 49.5
2		398.30	18.75
1	Proposed (NPC + CTR)	749.54	22.0 – 25.2
1 and 2		238.17	18.75

+ CTR) which utilizes much more compliant PC component as compared to other two structures. The same trajectories were tracked using the previous approach combined with NPC ([12]+NPC). The performance difference was not noticeable in terms of Cartesian position error, but the difference was significant in terms of stiffness of the PC components as seen in Fig. 6 and Table I.

In unstructured settings, it is safer to keep a low passive stiffness whenever applicable (i.e., lower PC stiffness) due to possible collisions, disturbances, or noise. This is especially true in dexterous manipulation with fragile objects. Note that sudden impacts or high frequency disturbances cannot be handled by controller stiffness due to the control delay and bandwidth of the system. Therefore, high frequency response reduces to the system’s passive dynamic response. With higher passive stiffness (i.e., higher PC stiffness), the system not only fails to passively reject high frequency disturbances but is also unable to render the desired stiffness, becoming more prone to damaging the environment or the robot itself because of its high passive stiffness. Therefore, utilizing a more compliant PC component to render the same desired stiffness is the safe, practical, and stiffness-efficient solution. With the previous approach [12] alone, we suspect that NuFingers would track the desired trajectory as well but at the expense of a very high stiffness.

On a side note, object manipulation in an elliptical path was more robust against higher controller stiffness compared to a

step response. We were able to reach above the robot’s passive stiffness in the elliptical path. This is because the frequency of the control input is much lower ($\sim 10^{-1}/s$) compared to the step input where oscillations are usually at a higher frequency ($\sim 10/s$). At lower frequencies and velocities, friction and stiction play a more important role to stabilize the system, and thus it is easier to reach stability [16][17].

IV. DISCUSSION

We presented a stiffness-efficient method of stabilization through passivity and demonstrated its positive effects via simulation and experiments. In the simulation, we assumed that there is no damping to better reflect the derived stability criteria. As expected, the proposed mechanism with NPC and CTR successfully stabilizes the system with minimal addition of stiffness. Using NuFingers, we carried out experiments further validating the efficacy of the proposed structure. Through three different scenarios, we verified the stabilization effects in an otherwise unstable system. After careful analysis, we make the following interesting observations.

A. Torque Requirements

The amount of torque required to overcome the passive stiffness element is profoundly different depending on the structure. Due to the absence of coupled tendon routing and use of the stiffer parallel compliance requirement for [12]+NPC, the size of the pulley is considerably larger than the proposed structure as shown in Fig. 7. Detailed moment arms

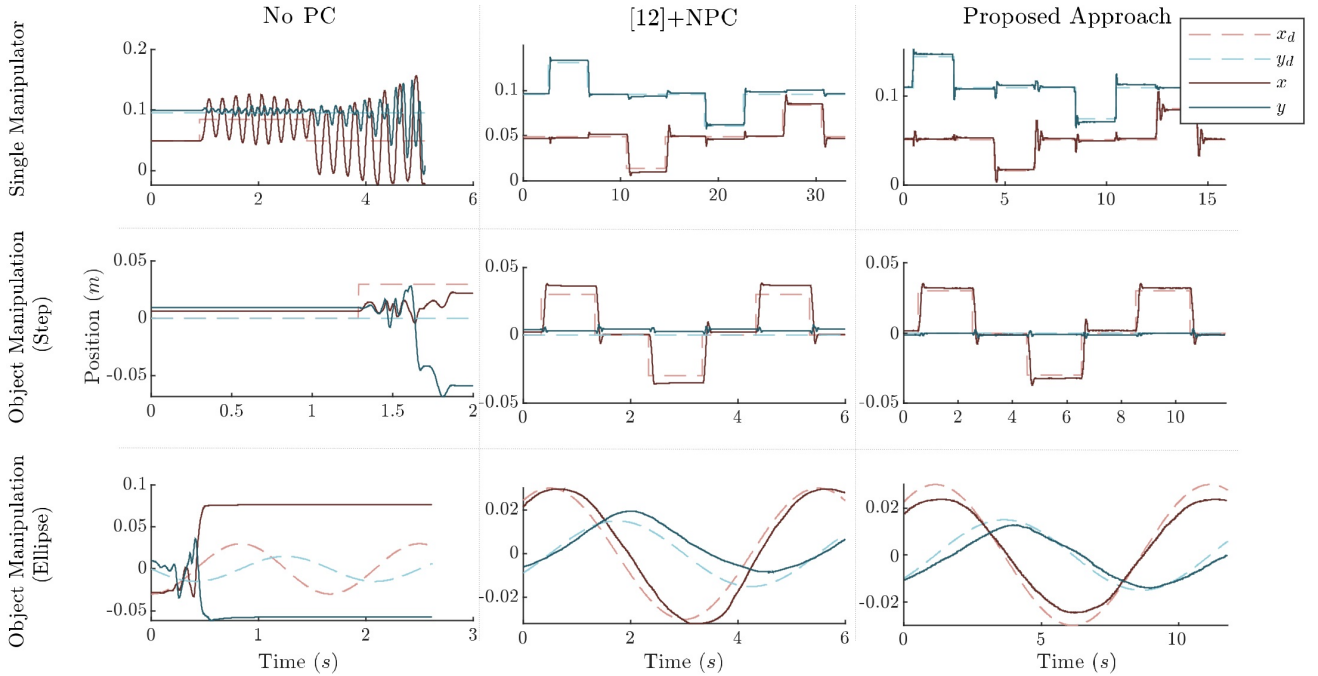


Fig. 8. Experiment results from the NuFingers setup are shown. In all cases, desired Cartesian stiffness is set high; $70 N/m$ in the case of a single manipulator and $140 N/m$ in the case of object manipulation. (Left) Without any PC, the system shows an oscillatory behavior or loses the grip on the object instantly. (Middle) With [12]+NPC, the system becomes stable at the expense of higher stiffness. (Right) With the proposed setup (NPC + CTR), the system maintains the overall passivity and stability even with significantly smaller overall stiffness. The steady-state error is due to unmodeled friction which shows to be more profound under low velocities. Regardless of the friction under low velocities in elliptical paths, the system without optimized PC cannot render the high stiffness.

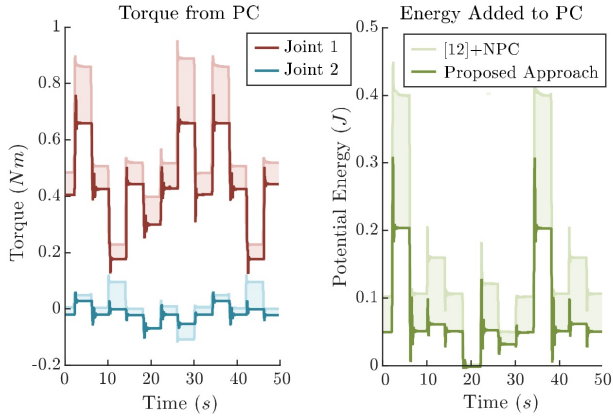


Fig. 9. The maximum restoring torques at the first joint and potential energy in PC elements show about 26% and 50% reduction respectively, in the proposed NPC + CTR setup (dark lines) compared to [12]+NPC (light lines). Potential energy was calculated according to the principle of virtual work. These plots demonstrate that the proposed setup can be much more efficient in terms of stiffness and torque requirements, and possibly also energy consumption, while preserving the overall passivity.

can be found in Table I. Therefore, the amount of torque and stiffness at the first joint differs in the two structures despite equal stiffness of the extension springs.

As mentioned before, torques originating from parallel compliance are fairly simple to calculate as they only depend on the configuration on the robot. Therefore, when controlling a robot with parallel compliance, one can simply add a feedforward term that would compensate for the restoring torques generated by the parallel compliance components. The restoring torques can be computed from integrating the stiffness curves from the corresponding equilibrium position, which are all known parameters in this work as shown in Eq. (4).

Figure 9 demonstrates that the maximum torque required to compensate for the restoring torques from PC has been reduced by up to 26% at joint 1 in Scenario 1. As a consequence, potential energy added to the PC elements also decreased by up to 50%. This suggests that incorporation of NPC and CTR can reduce the torque requirements greatly while maintaining a similar level of stability.

From the potential energy plots, we can further observe the possibility of energy expenditure reduction. This can be of great importance in fields of wearable platforms such as prostheses or exoskeletons, where power consumption is crucial to battery life. It is also known that reduction in required motor torques affects the size, weight, and cost of the actuation system. For example, it is easy to verify that nominal torque, size, weight, and cost of the motor all increase proportionally for commercialized DC motors [18]. In turn, the battery size can also be reduced, further lowering the weight.

In addition, the desired trajectories and the actuation mechanism remained the same across the experiments. Therefore the striking difference depicted in Fig. 9 is entirely due to the difference in stiffness for different physical structures as depicted in Fig. 6. Based on these figures and Table I, we

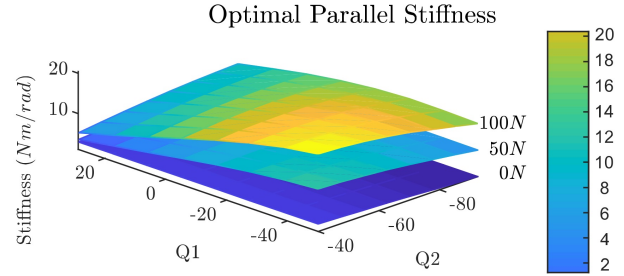


Fig. 10. The amount of coupling and nonlinearity becomes larger as the interaction force increases with respect to the desired stiffness. Top, middle, and bottom layers each show (1,1) element of optimal PC matrix across the workspace where interaction force is assumed to be 0N, 50N, and 100N respectively. Desired stiffness is all set to 150N/m. q_1 and q_2 represent joint positions.

can safely conclude that the previous approach [12] would result in higher torque demands due to higher stiffness, further requiring heavier actuation mechanisms.

B. Modeling Limitations

The nonlinear effects of stiction and damping on stability underscore shortcomings with classical passivity-based stability analysis. Formulation of the stability criteria does not take dynamic parameters such as damping and inertia into account [12]. This assumption makes the criteria a conservative measure of stability as more damping or inertia will help the system become stable. Indeed, we included no damping in the simulations.

However, in real-life applications, we cannot ignore inertia and damping as they contribute to the stability of the overall system. We have to take into account that the controller stiffness may be greater than the theoretical passive stiffness of the system, but the system can remain stable due to damping and inertial effects. Thus, to better reflect the stability criteria derived in Eq. (1), it is desirable to maintain experimental systems as frictionless and massless as possible.

C. Effects of Conservative Congruence Transformation Term

Throughout the optimization process, it is interesting to see that as the $\mathbf{K}_{j,CCT}$ term enlarges, the amount of coupling between the first and second joint that exists in $\mathbf{K}_{j,CCT}$ increases. This effect is illustrated in Fig. 10, suggesting that a single component of the optimal stiffness matrix is affected by the displacement of all joints. This effect is not as exaggerated in our experiments as depicted in Fig. 10 because the degree of this coupling effect depends on the ratio between the interaction force and the desired stiffness.

Thus, it is important to know the range of interaction forces required for a particular task before it is executed and whether the generated optimal stiffness covers the whole range. This plot also implies that if the interaction force changes, optimal stiffness changes along with it, even if the desired Cartesian stiffness stays constant. The interaction force affects the $\mathbf{K}_{j,CCT}$ term in Eq. (2). Therefore, it will be interesting to look for a new design that allows the stiffness to vary along with the interaction force.

V. CONCLUSIONS AND FUTURE WORKS

We have introduced the systematic optimization process of parallel compliance and demonstrated that stability of the system can be achieved from efficient and optimal design choices that lead to overall passivity. Through the usage of nonlinear parallel compliance (NPC) and coupled tendon routing (CTR) strategy, we have successfully reduced the overall stiffness of the parallel compliance components as compared to the previous approach [12]. Reduction of passive stiffness is not only beneficial in terms of power consumption, but also safer around unknown environments. The results demonstrated in this paper show the possibility of effectively shifting the stable stiffness range so the system meets the stiffness requirements throughout the given task while minimizing the overall stiffness. By being able to render various controller stiffnesses, the manipulator is able to handle a wider range of tasks that require different amounts of stiffness. The passive compliance is especially important when the robot moves in unstructured environments or manipulates objects with unknown kinematics and dynamics, as passive compliance aids robustness in unforeseen situations.

In addition to stiffness reduction, we have verified the relaxed torque requirements by using the proposed structure as compared to the previous approach. The torque requirements are computed through calculation of restoring joint torques based on the optimized \mathbf{K}_{pc} from Eq. (3). From the potential energy stored in the springs, we have seen the possibility of energy reduction which could be verified through further investigative experiments with batteries.

Benefits of implementing tendon-driven series elastic actuators include weight separation between the actuators and manipulators and thus usage of low capacity motors that drive the low inertia manipulators. Additionally, for high frequencies, the overall impedance of the system reduces to that of the physical springs, making the system a zero-delay low-pass filter. Introduction of the proposed structure with NPC and CTR opens up a new possibility of reducing the motor capacity and dropping the weight, size, and cost of the motors even further. This can be advantageous in the field of prostheses and exoskeletons. Furthermore, in such remote systems where battery life is crucial, energy-efficiency is an important factor to consider.

For future work, we hope to extend the current study in the following ways.

- Conduct experiments in mobile environments where the battery lifespan is crucial, and seek the feasibility and efficacy of the proposed structure in terms of robustness and energy efficiency.
- Extend the optimization methodology to include other design parameters such as link lengths, actuation pulley radii, routing strategies, etc.
- Investigate the optimization of coupled parallel compliance further to check feasibility of fully nonlinear and fully coupled parallel compliance components.

REFERENCES

- [1] Y.T. Lee, H.R. Choi, W.K. Chung, and Y. Youm. Stiffness Control of a Coupled Tendon-Driven Robot Hand. *IEEE Control Systems Magazine*, 14(5):10–19, 1994.
- [2] J. Pratt, B. Krupp, and C. Morse. Series elastic actuators for high fidelity force control. *The Industrial Robot*, 29(3):234–241, 2002.
- [3] C. Ott, A. Albu-Schaffer, A. Kugi, and G. Hirzinger. On the passivity-based impedance control of flexible joint robots. *IEEE Transactions on Robotics*, 24(2):416–429, 2008.
- [4] N.L. Tagliamonte and D. Accoto. Passivity constraints for the impedance control of series elastic actuators. *Proceedings of the Institution of Mechanical Engineers, Part I: Journal of Systems and Control Engineering*, 228(3):138–153, 2014.
- [5] G.A. Pratt and M.M. Williamson. Series elastic actuators. *IEEE/RSJ International Conference on Intelligent Robots and Systems*, 1995.
- [6] M. Zinn, O. Khatib, and B. Roth. A New Actuation Approach for Human Friendly Robot Design. *IEEE International Conference on Robotics and Automation*, 2004.
- [7] J. Morrell and J. Salisbury. Parallel-Coupled Micro-Macro Actuators. *The International Journal of Robotics Research*, 1998.
- [8] R. Ozawa, K. Hashirii, and H. Kobayashi. Design and Control of Underactuated Tendon-Driven Mechanisms. *IEEE International Conference on Robotics and Automation*, 2009.
- [9] T. Treratanakulwong, H. Kaminaga, and Y. Nakamura. Low-friction tendon-driven robot hand with carpal tunnel mechanism in the palm by optimal 3D allocation of pulleys. *IEEE International Conference on Robotics and Automation*, 2014.
- [10] M. Uemura, H. Goya, and S. Kawamura. Motion Control With Stiffness Adaptation for Torque Minimization in Multijoint Robots. *IEEE Transactions on Robotics*, 2013.
- [11] A.D. Deshpande, N. Gialias, and Y. Matsuoka. Contributions of Intrinsic Visco-Elastic Torques During Planar Index Finger and Wrist Movements. *IEEE Transactions on Biomedical Engineering*, 59(2):586–594, 2012.
- [12] P. Rao and A.D. Deshpande. Analyzing and Improving Cartesian Stiffness Control Stability of Series Elastic Tendon-Driven Robotic Hands. *IEEE International Conference on Robotics and Automation*, 2018.
- [13] S.F. Chen and I. Kao. Conservative Congruence Transformation for Joint and Cartesian Stiffness Matrices of Robotic Hands and Fingers. *The International Journal of Robotics Research*, 19(9): 835–847, 2000.
- [14] R.A. Waltz, J.L. Morales, J. Nocedal, and D. Orban. An interior algorithm for nonlinear optimization that combines line search and trust region steps. *Mathematical Programming*, 107(3):391–408, 2006.
- [15] B. Kim and A.D. Deshpande. Design of Nonlinear Rotational Stiffness Using a Noncircular Pulley-Spring Mechanism. *ASME Journal of Mechanisms and Robotics*, 6(4):041009, 2014.
- [16] Y.L. Yu and C.C. Lan. Design of a Miniature Series Elastic Actuator for Bilateral Teleoperations Requiring Accurate Torque Sensing and Control. *IEEE Robotics and Automation Letters*, 4(2):500–507, 2019.
- [17] W. Townsend and J. Salisbury. The Effect of coulomb friction and stiction on force control. *IEEE International Conference on Robotics and Automation*, 1987.
- [18] Maxon Motors Online Catalog. *Maxon Group*.